

Tumor growth modeling from clinical trials reveals synergistic anticancer effect of the capecitabine and docetaxel combination in metastatic breast cancer

N. Frances · L. Claret · R. Bruno · A. Iliadis

Received: 2 November 2010 / Accepted: 15 February 2011 / Published online: 8 April 2011
© Springer-Verlag 2011

Abstract

Purpose Most of the cancer chemotherapy treatments employ drugs in combination. For combination treatments, it is relevant to assess interaction between two or more anticancer agents used in clinics. Based on clinical data and using modeling techniques, the work analyzes the pharmacodynamic interaction between capecitabine and docetaxel used in combination in metastatic breast cancer.

Methods We developed mathematical models to describe tumor growth inhibition profile under treatment based on Phase II and Phase III clinical data of capecitabine and docetaxel in metastatic breast cancer. Model parameters were estimated by population approach with NONMEM[®] on single-agent and combination data. Simulations were performed using MATLAB.

Results Capecitabine and docetaxel combination in metastatic breast cancer results in a synergistic effect as compared with the simple additive effects of single-agent treatments. Docetaxel is more efficient than capecitabine at the start of treatment but develops resistance faster. Modeling revealed no resistance of capecitabine for the combination data.

Conclusions Modeling could be a powerful tool to design the most advantageous combination regimen for capecitabine and docetaxel in metastatic breast cancer in order to increase the time before regrowth and decrease the tumor size at regrowth.

Keywords Modeling · Interaction · Drug combination · Clinical data

Introduction

Combination therapy is widely used in the treatment of patients with cancer [1]. The main rationale to combine anticancer agents in the clinic is to obtain a better response while limiting adverse events. Combination trials are empirically designed on the basis of efficacy and safety data recorded from already performed single-agent studies. For the combination studies, it is relevant to assess interaction (synergistic, additive or antagonistic effect) between two or more anticancer agents.

Assessing the nature and intensity of combination drug therapy *in vitro* has been an interesting topic and many preclinical studies revealed challenging combinations of anticancer agents [2–5]. Roche developed capecitabine (*C*), an oral prodrug of fluorouracil which demonstrated efficacy in many cancers [6]. This oral treatment has obtained authorizations to be used as a single-agent or associated with taxanes, e.g., docetaxel (*D*) in metastatic breast cancer (MBC). Co-administration of *C* and *D* in xenograft models with colon cancer cellular lines resulted in synergistic antitumor activity [7]. The same combination was advocated for clinical trials in MBC. Data from single-agent chemotherapy [8, 9] were used to design the combination trial [8, 9]. Tumor size was monitored and investigators were free to modify administration protocols according to the severity of adverse events. The measurement of tumor size provided a continuous scale measure that was useful for describing the time course of tumor response in relation to drug administrations.

N. Frances · A. Iliadis (✉)
Department of Pharmacokinetics, UMR-MD3,
Faculty of Pharmacy, University of Méditerranée,
27, bld. Jean Moulin, 13385 Marseille cedex 5, France
e-mail: iliadis@univmed.fr

L. Claret · R. Bruno
Pharsight, A CertaraTM Company, Marseille, France

In this study, we used a population approach [10] to analyze the longitudinal tumor size data collected in Phase II and III studies [8, 9]. A pharmacodynamic model was established to describe tumor response to C and D used as single-agent or in combination. The objective was to assess interaction of drug combination.

Patients and methods

Patients, treatments

Clinical data regroups phase II and III clinical trials conducted as single-agent or combination treatments:

- The phase II trial assessed efficacy and safety of C as a single-agent [8].
- The phase III trial compared efficacy and safety of C plus D in combination versus D as a single-agent [9].

The following administration protocols were used:

- Single-agent treatment:
 - C in phase II (C database, 168 patients, 578 observations) administered in 3-week cycles twice daily at 2,510 mg/m²/d during 2 weeks and a 1-week rest period [8].
 - D in phase III (D database, 223 patients, 793 observations) administered at 100 mg/m² as a 1-hour intravenous infusion on the first day of each 3-week cycle [9].
- Combination treatment: C and D in phase III (C/D database, 222 patients, 897 observations). C was administered using the same dose and schedule as in the single-agent Phase II study. D was administered at 75 mg/m² as a 1-hour intravenous infusion on the first day of each 3-week cycle [9].

Patients achieving a complete or partial response or stable disease after 2 cycles of therapy continued on treatment until disease progression or development of unacceptable toxicity. Also, investigators were free to reduce drug doses or interrupt the treatment according to the severity of the adverse events.

Data

Tumor observations consisted in the sum of the longest diameters measured on metastatic sites. No covariates and no pharmacokinetic observations were available. The detailed dose administration protocol was available for each patient.

Before data processing, the available database was cleaned from records inconsistent with the study design or administration protocol or when the administration

protocol was not documented. So, 22 patients overall and 18 observations from 10 patients were removed from the 3 databases. The final C , D , and C/D databases contain 571, 749, and 809 observations for 167, 216, and 208 patients, respectively. At total 2,129 observations over 591 patients were analyzed with less than four observations available per patient at average.

Modeling

Because there was no pharmacokinetics data, the dose history was introduced in the tumor growth model by means of a K/PD model [11]:

$$\begin{aligned}\frac{dC(t)}{dt} &= -k_C \cdot C(t) + u_C(t)C(0) = 0 \\ \frac{dD(t)}{dt} &= -k_D \cdot D(t) + u_D(t)D(0) = 0\end{aligned}\quad (1)$$

In these equations, $C(t)$ and $D(t)$ are the dose histories for C and D , respectively. Parameters k_C and k_D called “biologic constants” control the dose history profiles. Functions $u_C(t)$ and $u_D(t)$ describe schedules and amounts of administration protocols. The K/PD model captures time delay effect on tumor like models as already proposed by others [12]. Also, it allows accounting for any accumulation of the effect with time.

To describe the action of each drug on the tumor cells, time-varying cell-kill rates were to account for drug resistance, as a mechanism modifying cell-kill rates according to an exponential time decline. Thus, the cell-kill rates $f_C(t)$ and $f_D(t)$ for C and D , respectively, were:

$$\begin{aligned}f_C(t) &= p_C \cdot \exp(-\rho_C \cdot t) \cdot C(t) \cdot n(t) \quad \text{and} \\ f_D(t) &= p_D \cdot \exp(-\rho_D \cdot t) \cdot D(t) \cdot n(t)\end{aligned}\quad (2)$$

In these expressions, $n(t)$ denotes the tumor size, p_C and p_D are the efficacy rates of the drugs, and ρ_C and ρ_D are the resistance parameters.

The tumor size dynamics $n(t)$ was described by the following differential equation:

$$\frac{dn(t)}{dt} = f_+(t) - f_-(t) \quad n(0) = n_0 \quad (3)$$

involving two competing terms; tumor proliferation $f_+(t)$ and tumor shrinkage $f_-(t)$ rates due to the cell-kill rates of both drugs:

$$f_-(t) = f_C(t) + f_D(t). \quad (4)$$

The tumor size at the start of treatment was denoted n_0 . The function $f_+(t)$ is a Gompertz growth model with proliferation rate denoted λ and maximum tumor burden θ fixed at 1,000 mm:

$$f_+(t) = \lambda \cdot \ln \left[\frac{\theta}{n(t)} \right] \cdot n(t) \quad (5)$$

In the above models, k_C , k_D , λ , n_0 , p_C , p_D , ρ_C , and ρ_D are parameters to be estimated given the observed data.

Data analysis

Tumor sizes were analyzed according to the population approach [10]. The study was only focused on the description of the population characteristics (post-hoc estimation of individual parameters was out of the scope). The first-order conditional estimation method with interaction (FOCE-I) in NONMEM (v6 Globomax LLC, Hanover, USA) was used to estimate population parameters. Interindividual variability was assumed to follow exponential models involving fixed effect parameters, typical for the population considered, and random effect parameters describing differences between individuals. The random components in the exponential model are assumed to have zero mean and variance ω^2 . Residual errors were considered as proportional having zero mean and variance σ^2 .

In an exploratory study [13], several modeling structures were tested with different types of tumor growth and different types of cell-kill rates, common or individual resistance terms to C and D , etc. The Akaike Information Criterion (AIC) was employed to discriminate candidate models. Bootstrap resampling technique was applied as an internal validation tool to assess the final population parameter estimates. Two hundred bootstrap replicates were generated by randomly resampling the original data set with replacement. The median values and 95% confidence intervals of these 200 bootstrap replicates were compared with the estimates from the original data set.

To compare combination versus single-agent treatments, simulations were performed involving the same model (Eqs. 1, 3) using either the parameters estimated from combination (“ C/D ” case) or those from single-agent data (“ $C + D$ ” case) analyses. Comparisons were made on the tumor shrinkage rate $f_-(t)$, on the regrowth time, and on the tumor size at the regrowth time. The regrowth time is defined as the time just before tumor regrowths. The regrowth time and the tumor size at regrowth time are computed for several scenarios involving variable dose reductions beyond the 3rd cycle of treatment. For the “ C/D ” case, comparisons were also made between $f_C(t)$ and $f_D(t)$ cell-kill rates. Since the three population analyses cannot be matched to obtain pairwise comparisons, only the average behavior associated with its 95% confidence interval was provided for the above quantities. Approximate 95% confidence intervals for the average behavior were calculated by:

$$\bar{x} \pm 1.96 \cdot \frac{s}{\sqrt{n}}$$

where s and \bar{x} are the sample standard deviation and the sample mean, respectively. These statistics were obtained

from 1,000 samples drawn randomly from each population analysis. Simulations were performed using MATLAB v8a environment [14].

Results

“Biologic constants” in the K/PD model were estimated from single-agent data without random components. They were subsequently fixed in the model analyzing the combination data assuming that “biologic constants” were not modified by combining drugs. Whatever the treatment (single-agent or combination), the final model was obtained without random component for resistance parameters. For the combination data, modeling revealed resistance for D but not for C . Table 1 summarizes the population parameter estimates with the associated standard errors. For the combination data, Fig. 1 shows the distribution of bootstrap replicates. The reported 95% confidence intervals include estimates from the original data and so validate the population estimates of model parameters. The same validation was performed for the single-agent population data (results not presented).

Literature reports no pharmacokinetic interaction between C and D [15]. Therefore, any difference in response between “ C/D ” and “ $C + D$ ” cases was assumed to be due to a pharmacodynamic interaction. Data presented in Table 1 were obtained with fixed values for “biologic constants” at $k_C = 0.6 \text{ w}^{-1}$ and $k_D = 0.2 \text{ w}^{-1}$. Even without covariates, residual variability remained at moderate levels (24.6, 28.3, and 26.2% for the 3 databases) and the largest interindividual variability did not exceed 77% (reported for λ). Interindividual variabilities for p_C and p_D did not exceed 57% and they were the lowest over all parameters in the model. Initial tumor sizes and associated interindividual variabilities were similar for the 3 databases. Single-agent databases revealed that D was more efficient ($p_D = 3.34 \cdot 10^{-1}$ vs. $p_C = 1.22 \cdot 10^{-3} \text{ g}^{-1} \text{ w}^{-1}$) but developed resistance faster ($\rho_D = 8.76 \cdot 10^{-2}$ vs. $\rho_C = 4 \cdot 10^{-2} \text{ w}^{-1}$) than C . The efficacy p_C was lower in combination than in single-agent treatment ($9.68 \cdot 10^{-4}$ vs. $1.22 \cdot 10^{-3} \text{ g}^{-1} \text{ w}^{-1}$) but in combination, modeling revealed no resistance of C . These findings were further explored in the following simulations.

Simulated time profiles presented in Figs. 2, 3, and 4 were obtained for a typical patient of 1.75 m^2 under the usual “ C/D ” protocol with initial C and D doses of 4.4 g/d and 132 mg , respectively. These doses were maintained unchanged along the treatment. However, because of toxicity, only few patients maintained the initial full C dosing scheme and when it happened, only for a short period of time.

Table 1 Estimation and standard errors in % (SE) of population parameters from *C*, *D*, and *C/D* databases

	<i>C</i>		<i>D</i>		<i>C/D</i>	
	Estimate	SE (%)	Estimate	SE (%)	Estimate	SE (%)
λ (w^{-1})	4.65E-3	33.1	6.26E-3	24.7	7.98E-3	17.3
n_0 (mm)	61.2	5.57	55.5	5.00	56.0	4.80
p_C ($g^{-1} w^{-1}$)	1.22E-3	22.6	NA	NA	9.68E-4	27.5
p_D ($g^{-1} w^{-1}$)	NA	NA	0.334	17.1	0.460	16.3
ρ_C (w^{-1})	4.00E-2	31.5	NA	NA	NE	NE
ρ_D (w^{-1})	NA	NA	8.76E-2	19.7	7.46E-2	24.5
ω^2 (λ)	0.592	31.9	0.470	26.6	0.422	18.8
ω^2 (n_0)	0.470	11.3	0.481	9.98	0.449	10.1
ω^2 (p_C)	0.326	29.7	NA	NA	0.233	53.6
ω^2 (p_D)	NA	NA	0.288	16.6	0.270	32.7
σ^2	6.04E-2	12.2	8.02E-2	12.1	6.89E-2	10.7

NA not applicable, NE not estimated. Parameters λ and n_0 are the proliferation rate and the tumor size at the start of treatment, respectively. Parameters p_C and p_D are the efficacy rates of the drugs, and ρ_C and ρ_D are the resistance parameters. The variances associated to the interindividual variability and to the residual error are denoted ω^2 and σ^2 , respectively; they are free of measurement units

For these analyses, biological constants were fixed at $k_C = 0.6 w^{-1}$ and $k_D = 0.2 w^{-1}$

Fig. 1 Distribution of the 200 bootstrap replicates. Estimates from the combination original data set (*thick vertical line*) and 95% confidence intervals of bootstrap replicates (from up *left-hand side* to *bottom right-hand side* successively for parameters λ , p_C , p_D , ρ_D , and n_0)

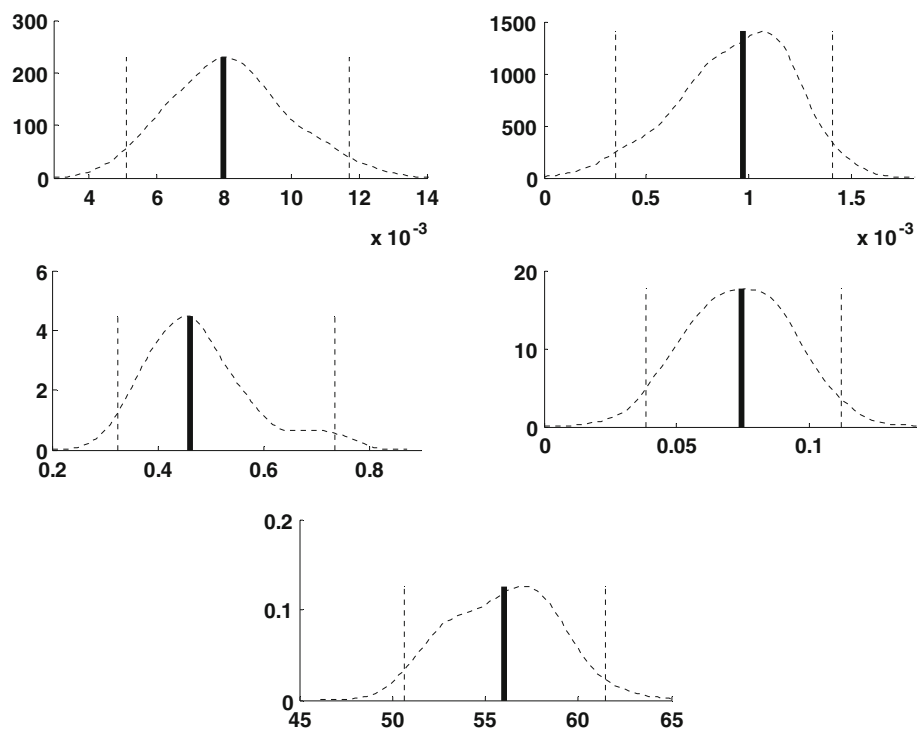


Figure 2 presents the average tumor size $n(t)$ profile with its confidence interval in the “*C/D*” case. The average tumor size profile was obtained with initial tumor size of 70.7 mm. The tumor achieved its minimum size (28.6 mm) 30.5 weeks after the start of treatment and then it began to regrowth because of resistance (i.e., regrowth time and

tumor size at the regrowth time were 30.5 w and 28.6 mm, respectively).

Figure 3 presents the average tumor shrinkage rate $f_-(t)$ and its 95% confidence intervals for “*C/D*” and “*C + D*” cases. Since $f_-(t)$ depends on “biologic constants” (k_C , k_D), on efficacy (p_C , p_D), and on resistance parameters (ρ_C ,

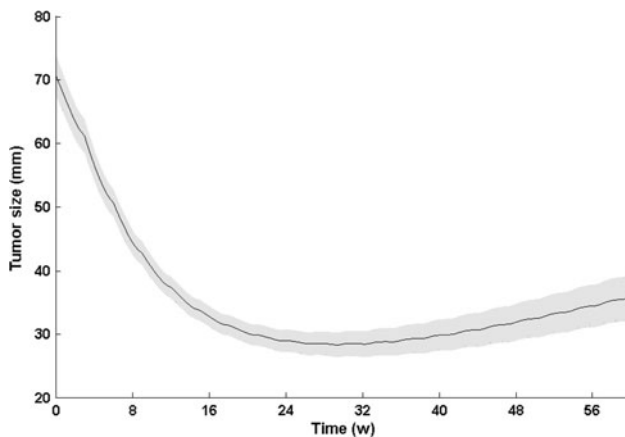


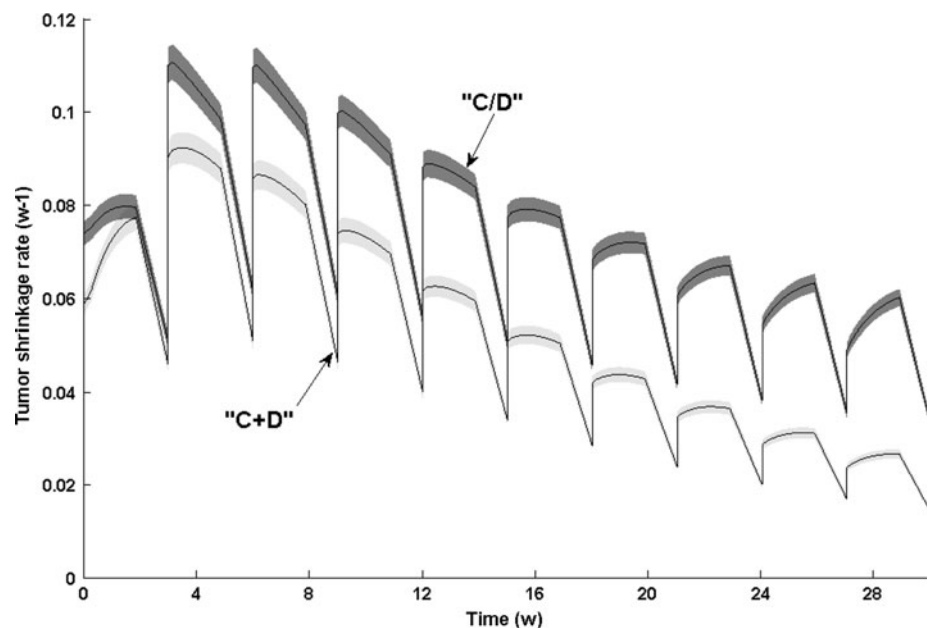
Fig. 2 Average tumor size $n(t)$ profile with its 95% confidence interval for the “C/D” case

ρ_D), $f_-(t)$ expresses somewhat the overall efficacy of the conducted therapy. $f_-(t)$ profiles confirmed the higher efficacy of the combination; the average $f_-(t)$ profile in “C/D” case was significantly ($P < 10^{-4}$) higher than in “C + D” case.

In the “C/D” case, Fig. 4 presents the average cell-kill rates $f_C(t)$ and $f_D(t)$ and their 95% confidence intervals. $f_C(t)$ and $f_D(t)$ profiles showed that D was more efficient than C at the start of treatment. Then, D efficacy was down-regulated because of resistance and C became more efficient than D after 4 months of treatment.

The regrowth time and the tumor size at the regrowth time were computed by assuming that the initial protocol was administered for the 3 first cycles and then the doses of C and D were reduced once according to a factor ranging between 1 and 0.5. Figure 5 shows the average regrowth time computed for each pair of values of factors of dose

Fig. 3 Average tumor shrinkage rate $f_-(t)$ with its 95% confidence intervals for the “C/D” (black) and “C + D” (gray) cases



reduction for C and D . It was significantly ($P < 10^{-4}$) longer in the “C/D” than in the “C + D” case. Similarly, the average tumor size at the regrowth time was significantly ($P < 10^{-4}$) lower in the “C/D” than in the “C + D” case (confidence intervals not presented). These findings illustrate the synergistic effect of combination treatment and confirm the above discussion on parameters estimates.

Discussion

Available databases were obtained in order to assess efficacy and therefore validate treatments including C and D as single-agent or combination chemotherapies. To assess efficacy, modeling of the observed tumor time course was developed. Investigators were authorized to empirically modify the drug doses in relation to the recorded adverse events [8, 9]. This practice constitutes an empirical alternative to the procedures involving mathematical modeling, Bayesian parameter estimation and dose individualization [16].

Modeling of drug interactions was recently attempted on preclinical data [2–5]. In parallel, some works reported tumor growth inhibition modeling but from single-agent clinical studies [17] and only a brief report analyzed drug combination data from clinical trials [18]. Working with the same data, the developed model in this study revised the dosing history and the resistance description used in [18].

From the estimated population parameters (Table 1), the association of higher efficacy p_D with slower resistance ρ_D in the combination compared with the single-agent treatment would indicate enhanced efficacy of D when

Fig. 4 Average cell-kill rates $f_C(t)$ and $f_D(t)$ with their 95% confidence intervals for C and D , respectively

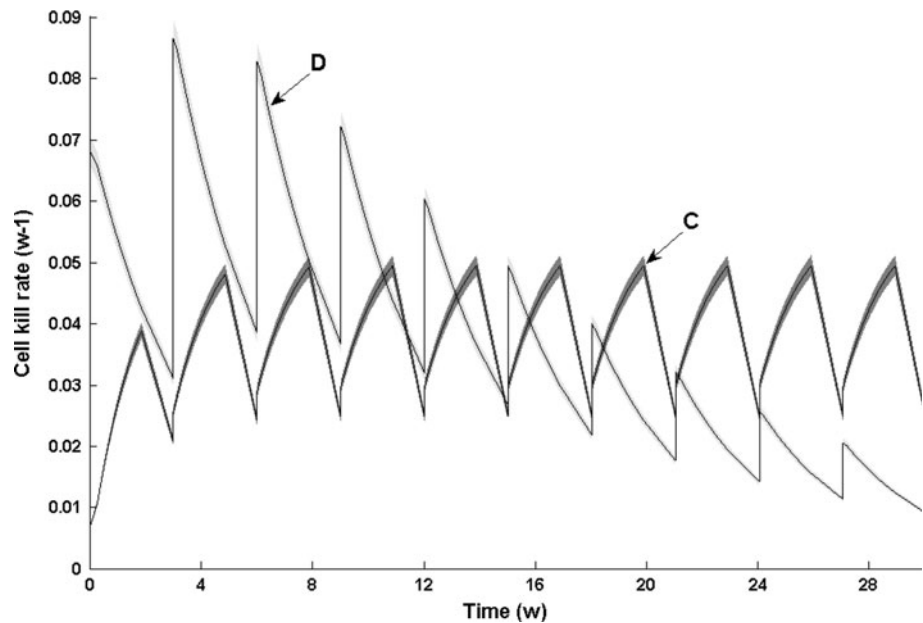
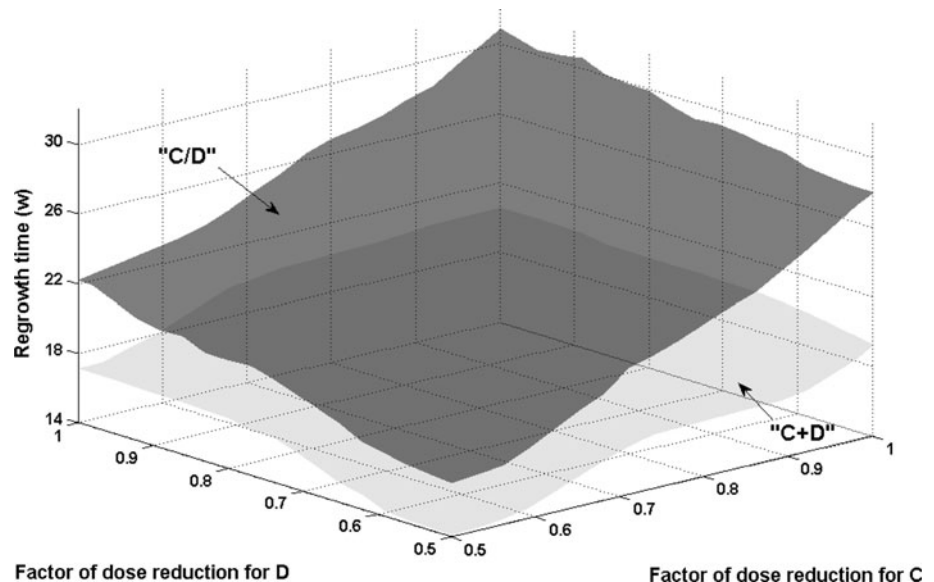


Fig. 5 Average regrowth time for the “ C/D ” (up mesh) and “ $C + D$ ” (down mesh) cases. The horizontal plane defines all combinations of the factors of dose reductions for C and D and the vertical axis expresses the corresponding average regrowth time



combined with C . Moreover, simulations (Fig. 3) revealed that pharmacodynamic interaction enhances the efficacy of drug combination as compared with the efficacy obtained by adding single-agent drug effects. Consequently, the combination of C with D leads to a synergistic (more than additive) effect.

C and D could be characterized as “complementary” agents since D was more efficient than C at the start of treatment and then, because of the D resistance, C became more efficient than D (Fig. 4).

The regrowth time is similar to the time to progression [19] usually reported in cancer clinical trials. In association with the tumor size at the regrowth time, it characterizes the balance on the average tumor size profile between

tumor growth and drug action mechanisms. As expected, higher dose schemes resulted in prolonging the regrowth time (Fig. 5) and in decreasing the tumor size at the regrowth time whatever the case (“ $C + D$ ” or “ C/D ”). On the other hand, Fig. 5 shows that regrowth time was more sensitive to C rather to D dose variations. Then, prolongation of the regrowth time could be achievable by higher C doses, if adverse events allow it.

The developed model from population analyses of the single-agent and combination databases may help to design better clinical trials. It could be used to design combination trials from analysis of single-agent databases. In a parallel study [13], we found that population parameters can be reliably estimated from a smaller number of patients from

the *C/D* database (e.g., as one would obtain in a phase II study). So, the model developed from combination databases over a limited number of patients (phase II clinical trial) could be used to design the combination protocol for subsequent phase III clinical trials (larger number of patients).

Conclusion

Population analysis of clinical trial databases led to three major conclusions. First, *C* and *D* combination in MBC results in a synergistic effect as compared with the simple additive effects of single-agent treatments. Second, *D* is more efficient than *C* at the start of treatment but develops resistance faster. Third, modeling revealed no resistance of *C* for the combination data. On the basis of efficacy, *C* and *D* could be characterized as “complementary” agents. These findings could be used to anticipate and design the combination treatment.

Modeling was used in population approaches to describe the impact of the anticancer treatment on the dynamics of tumor growth under single-agent and combination chemotherapy for MBC. This model captured the complex aspects of a combination therapy, it quantified *in vivo* the drug interaction and it evaluated the interindividual variability across patients. So, this approach could be a powerful tool to select the most advantageous combination therapies or to design more efficient and safer new administration protocols. A basic methodology was already established for optimizing the single-agent regimen minimizing the tumor burden while limiting toxicity [20]. For several drugs in combination, a methodology is currently under development. It aims to optimize the scheduling of drug administrations and compute dose modifications during the cycle of chemotherapeutic treatment.

Acknowledgments The authors thank Ms. Franziska Schaedeli-Stark of Pharma Research and Early development, Translational Research Sciences, Modeling and Simulation, F. Hoffmann-La Roche, Basel, Switzerland for her helpful comments and suggestions.

References

- Frei E (1972) Combination cancer therapy: presidential address. *Cancer Res* 32(12):2593–2607
- Koch G, Walz A, Lahu G, Schropp J (2009) Modeling of tumor growth and anticancer effects of combination therapy. *J Pharmacokinet Pharmacodyn* 36(2):179–187
- Rocchetti M, Bene FD, Germani M, Fiorentini F, Poggesi I, Pesenti E, Magni P, Nicolao GD (2009) Testing additivity of anticancer agents in pre-clinical studies: a PK/PD modelling approach. *Eur J Cancer* 45(18):3336–3346
- Schicher N, Paulitschke V, Swoboda A, Kunstfeld R, Loewe R, Pilarski P, Pehamberger H, Hoeller C (2009) Erlotinib and bevacizumab have synergistic activity against melanoma. *Clin Cancer Res* 15(10):3495–3502
- Goteti K, Garner C, Utley L, Dai J, Ashwell S, Moustakas D, Gönen M, Schwartz G, Kern S, Zabludoff S, Brassil P (2010) Preclinical pharmacokinetic/pharmacodynamic models to predict synergistic effects of co-administered anti-cancer agents. *Cancer Chemother Pharmacol* 66(2):245–254
- Walko C, Lindley C (2005) Capecitabine: a review. *Clinical Therapeutics* 27(1):23–44
- Sawada N, Ishikawa T, Fukase Y, Nishida M, Yoshikubo T, Ishitsuka H (1998) Induction of thymidine phosphorylase activity and enhancement of capecitabine efficacy by taxol/taxotere in human cancer xenografts. *Clin Cancer Res* 4(4):1013–1019
- Blum J, Jones S, Buzdar A, Lorusso P, Kuter L, Vogel C, Osterwalder B, Burger H, Brown C, Griffin T (1999) Multicenter Phase II study of capecitabine in paclitaxel-refractory metastatic breast cancer. *J Clin Oncol* 17(2):485–493
- O’Shaughnessy J, Miles D, Vukelja S, Moieseyenko V, Ayoub J, Cervantes G, Fumoleau P, Jones S, Lui W, Mauriac L, Twelves C, Hazel G, Verma S, Leonard R (2002) Superior survival with capecitabine plus docetaxel combination therapy in anthracycline-pretreated patients with advanced breast cancer: Phase III trial results. *J Clin Oncol* 12(12):2812–2823
- Beal S, Sheiner L (1980) The NONMEM system. *Am Stat* 34(2):118–119
- Jacqmin P, Snoeck E, Schaick EV, Gieschke R, Pillai P, Steimer J, Girard P (2007) modelling response time profiles in the absence of drug concentrations: definition and performance, evaluation of the K–PD model. *J Pharmacokinet Pharmacodyn* 34(1):57–85
- Mager D, Wyska E, Jusko W (2003) Diversity of mechanism-based pharmacodynamic models. *Drug Metab Dispos* 31(5): 510–518
- Frances N, Claret L, Stark FS, Bruno R, Iliadis A (2008) Modeling of longitudinal tumor size data in clinical oncology studies of drugs in combination. PAGE, Marseille
- MATLAB (2008) High-performance numeric computation and visualization software. R2008.a edn. The Math Works, Natick MA
- Prnk L, Vasey P, Sparreboom A, Reigner B, Planting A, Gordon R, Osterwalder B, Verweij J, Twelves C (2000) A phase I and pharmacokinetic study of the combination of capecitabine and docetaxel in patients with advanced solid tumours. *Br J Cancer* 83(1):22–29
- DeJonge M, Huitema A, Schellens J, Rodenhuis S, Beijnen J (2005) Individualised cancer chemotherapy: strategies and performance of prospective studies on therapeutic drug monitoring with dose adaptation: a review. *Clin Pharmacokinet* 44(2): 147–173
- Tham LS, Wang L, Soo RA, Lee SC, Lee HS, Yong WP, Goh BC, Holford NH (2008) A pharmacodynamic model for the time course of tumor shrinkage by gemcitabine + carboplatin in non-small cell lung cancer patients. *Clin Cancer Res* 14(13): 4213–4218
- Claret L, Girard P, Zuideveld K, Jorga K, Fagerberg J, Bruno R (2006) A longitudinal model for tumor size measurements in clinical oncology studies. PAGE, Bruges, Belgium
- Durie B, Jacobson J, Barlogie B, Crowley J (2004) Magnitude of response with myeloma frontline therapy does not predict outcome: importance of time to progression in southwest oncology group chemotherapy trials. *J Clin Oncol* 22(10):1857–1863
- Iliadis A, Barbolosi D (2000) Optimizing drug regimens in cancer chemotherapy by an efficacy-toxicity mathematical model. *Comput Biomed Res* 33(3):211–226